
Faculty of Engineering and Computer Science

Faculty Publications

This is a post-print version of the following article:

Threshold for Terahertz Resonance of Nanoparticles in Water

Dao Xiang, Jian Wu, Jörg Rottler and Reuven Gordon

2016

The final publication is available at:

<https://doi.org/10.1021/acs.nanolett.6b00770>

Citation for this paper:

Xiang, D., Wu, J., Rottler, J., & Gordon, R. (2016). Threshold for Terahertz Resonance of Nanoparticles in Water. *Nano Letters*, 16(6), 3638–3641.

<https://doi.org/10.1021/acs.nanolett.6b00770>

Threshold for Terahertz Resonance of Nanoparticles in Water

Dao Xiang,¹ Jian Wu,¹ Jörg Rottler,² Reuven Gordon^{*1}

¹Department Electrical and Computer Engineering, University of Victoria, Victoria, BC V8P 5C2, Canada

²Department of Physics and Astronomy, University of British Columbia, Vancouver, BC V6T 1Z1, Canada

ABSTRACT: Nanoparticle vibrations are coupled to light through electrostriction, which gives nonlinear optical scattering. We investigated the acoustic response of 2 nm gold nanoparticles using nearly-degenerate four-wave mixing experimental configuration and show that the nonlinear response suddenly turns on at low powers (<100 mW) for continuous-wave (CW) lasers. The observed nonlinear response is a million times larger than typical electronic nonlinearities. The threshold implies a dramatic change in the quality factor of the vibrating nanoparticles, 4 orders of magnitude larger than usual hydrodynamic theory predicts. It is as if the water is removed altogether, which we speculate is the result of the vibrating particle pushing away the water molecules to form a stable cavity. Since these acoustic vibrations extend to terahertz frequencies, there is potential to harness this effect for high speed optical data processing; as well as to probe the dynamics of proteins all having acoustic modes in this range.

KEYWORDS: *Four-wave mixing, Electrostriction, Terahertz, Acoustics, Cavitation, Nanoparticles*

There has been a long history of studying the optically driven acoustic response of nanoparticles, providing the fundamental insight into the elastic properties of nanometer-size objects. Conventionally, damping from the surrounding medium limits the nonlinear response, so past investigations have been limited to using high peak intensity ultrafast lasers¹⁻¹². In solid materials, these oscillations are usually critically damped and provide only a small change in the optical scattering¹³. Similar experiments in solution still used high peak power femtosecond lasers to show an appreciable damping³, with quality factors of the order of 10-100. The application of high-sensitivity sensors reaching the terahertz range spurs considerable research interest in the nanoscale systems, while it holds the demanding requirement in the sufficiently high quality factor⁴. Similarly, femtosecond optical Kerr-effect spectroscopy has been used to study the terahertz dynamics of proteins in solution¹⁴, with quality factors below 10 observed. Here we show the unexpected result that even a weak laser can generate extraordinarily strong four-wave mixing (FWM) signal above a critical threshold intensity. This finding suggests extremely high quality factors for the nanoparticle vibrations, as if the water damping disappears entirely.

We use four-wave mixing to probe the nonlinear response of dilute gold nanoparticles in solution. A schematic of the setup is shown in Figure 1. This setup is similar to degenerate four-wave mixing experiments that used gradient forces to create strong refractive index changes in degenerate four-wave mixing¹⁵; however, we use an external cavity laser (ECL) (DL100, Toptica Photonics), and a distributed Bragg reflector (DBR) laser (DBR852P, Thorlabs) tuned to slightly different wavelengths to obtain non-degenerate response. The nonlinear medium was an aqueous suspension of 2 nm diameter gold nanoparticles (EM.GC2, BBI Solutions) centrifuged at 1200 rpm to increase the concentration to 6.3×10^{-6} volume fraction. The polarization controller and polarizer ensured co-polarized illumination. The angle between the laser beam with amplitude A_1 and the laser beam with amplitude A_3 was adjusted to 4° to allow over 1 mm light-matter interaction length (the length of the cuvette was 1 mm). Weak focusing lenses were used with focal lengths of 20 cm and 4 cm. The optical chopper modulated the intensity of one pump beam to only permit the Rayleigh scattered light of that pump and the FWM beam from the counter-directional beam to be measured by an avalanche photodetector (APD120A, Thorlabs) when using a lock-in amplifier (SR510, Stanford Research Systems). The power of the DBR laser was fixed to 25 mW to limit the amplitude of Rayleigh scattered light, while the power of external-cavity laser was set to a relatively high value of 67 mW (total) to excite two beams of the four-wave mixing process. The frequency difference between the two laser sources was scanned with the step of 3 GHz by temperature tuning the DBR laser. A variable optical attenuator after the external-cavity laser output was used to obtain the power dependence of nonlinear response at acoustic resonance. We observe four-wave mixing peaks at 504 GHz and 1.511 THz at 67 mW for the ECL and 25 mW for the DBR, as shown in Figure 2. The free space vibrational resonances predicted by Lamb's theory¹⁶ are 508 GHz and 1.518 THz for the $l=2$ and 0 resonances, with the longitudinal sound velocity of 3240 m/s and transverse sound velocity of 1200 m/s¹⁷.

The manufacturer specifies smaller than 8% dispersion in particle size. For comparison, Figure 2 shows also this variation in grey. It is clear from this that the experimentally observed linewidth of the resonant response is within the specified dispersion. This suggests that inhomogeneous broadening is the dominant factor in the observed linewidth.

From the power detected in the FWM setup, we estimate the third-order susceptibility $\chi^{(3)}$ to be $1.6 \times 10^{-16} \text{ m}^2 \text{V}^{-2}$ and $0.9 \times 10^{-16} \text{ m}^2 \text{V}^{-2}$ corresponding to the $l = 2$ resonance and $l = 0$ resonance respectively by solving the coupling-wave equations in nonlinear optics¹⁸:

$$I_4 \approx |\kappa|^2 L^2 I_3 = \left(\frac{3\pi}{\epsilon_0 n_s^2 c \lambda} |\chi^{(3)}| \right)^2 L^2 I_1 I_2 I_3 \quad (1)$$

where ϵ_0 is vacuum permittivity, n_s is refractive index of water, c is the optical velocity in free-space, λ is the optical wavelength, I_i is the optical current for the beam i ($i = 1, 2, 3, 4$) (see Supporting Information for details). This is approximately a million times larger than the typical electronic response of condensed matter¹⁸. Of course, it should be noted that the nanoparticle solution is dilute, with the volume fraction of nanoparticles being 6.3×10^{-6} . Also, there is negligible extinction in the probed length. Therefore, a nonlinear susceptibility of $10^{-12} \text{ m}^2 \text{V}^{-2}$

possible by simply increasing the particle density to 7%. For this value, the calculated extinction is still very low at 0.1 cm^{-1} due to the small size of the nanoparticles and the near-IR working wavelength.

We observe a threshold in the power dependence of the observed FWM response, as shown in Figure 3. The threshold is at 43 mW for the $l = 2$ resonance, and at 55 mW for the $l = 0$ resonance. Below this threshold, there is negligible FWM signal. Above the threshold, the signal increases with the ECL power. The power dependence is between linear and quadratic. FWM would suggest a quadratic dependence on the ECL beam since it contributes two of the waves; however, the threshold dependence suggests that the nonlinear effect abruptly turns on, and so a simple quadratic scaling may not apply.

The viscoelastic theory¹⁹ for the water predicts that the $l = 2$ resonance occurs at 492 GHz with a quality factor of 7, and that the $l = 0$ resonance occurs at 1.487 THz with a quality factor of 14. These values are not in as good agreement as conventional Lamb's theory for a sphere in vacuum. Also, the quality factors suggest too much damping to achieve a strong nonlinear response. (A table in the Supporting Information summarizes these values).

One possible explanation of the observed threshold is the intrinsic threshold behavior of the nonlinear scattering. The setup considered here has a positive detuning of the tunable laser, which corresponds to stimulated Raman scattering (however, the basic physical mechanism is electrostriction, and this is common to the phenomena of acoustic Raman scattering, stimulated Brillouin scattering and four-wave mixing). Using the generic formulation for $\chi^{(3)}$, the threshold gain parameter for $l=2$ mode is calculated as

$$G_{th} = |\kappa_{th}|L = \frac{3\omega}{2\varepsilon_0 n_s^2 c^2} |\chi^{(3)}| \sqrt{I_{1cr} I_2} L \approx 0.002 \quad (2)$$

where $\omega=2.2 \times 10^{15} \text{ rad/s}$, $\varepsilon_0=8.85 \times 10^{12} \text{ F/m}$, $n_s=1.33$, $c=3 \times 10^8 \text{ m/s}$, the critical intensity $I_{1cr}=1.37 \times 10^6 \text{ W/m}^2$, the DBR laser intensity $I_2=1.69 \times 10^7 \text{ W/m}^2$, $L=1 \text{ mm}$. Although an exceedingly large $\chi^{(3)}$ is used in this estimation of G_{th} , the value is four orders of magnitude smaller than the threshold required for stimulated Brillouin scattering¹⁸ and stimulated Raman scattering²⁰. Therefore, we can believe that those other mechanisms cannot alone explain the observations.

Another possible explanation of the observed threshold dependence and the strong nonlinear response is the formation of a cavity or bubble around the oscillating nanoparticles. When electrostriction driving the particle motion is strong enough, the water molecules will be pushed away. Using the experimentally measured FWM signal, the amplitudes of $l=2$ and $l=0$ vibrational modes are 3 pm and 1.4 pm at the maximum pump intensity (see Supporting Information for details). The time to collapse over this distance for a bubble of radius equal to the nanoparticle radius can be given by integration of the Rayleigh-Plesset equation²¹. Integrating this equation, we find that the collapse times of 4.3 ps and 2 ps for the $l=2$ and $l=0$ vibrational modes. These are larger than the oscillation periods, so this may be viewed as the threshold condition to obtain oscillation with low damping. That is, to maintain a stable bubble that does not collapse. Considering Debye theory and permittivity measurements of water, the collision rate for water is around 20 GHz²³. For oscillations faster than this rate, the nanoparticle pushes away the molecules before they experience significant damping and a displaced water molecule cannot

return within one period of oscillation, so that a stable cavity may form. The displacement, however, is of the order of picometers, and so a very small “bubble” is expected to form. This mechanism may be analogous to the usual acoustic cavitation in low-pressure regions of water excited with acoustic waves²⁴; however, since we are considering high frequency and small scale oscillations, molecular dynamics simulations may be more appropriate²⁵ (see Supporting Information for preliminary molecular dynamics simulations). We rule out the possibility of plasmonic heating because the lasers are away from the plasmonic resonance and the response is clearly related to the acoustic vibrations.

We can consider how electrostriction theory relates to the observed nonlinear response and the expected damping. We estimate that the quality factor of the resonance scales as:

$$Q = \frac{y(\omega_a)}{y(0)} \quad (3)$$

where y is the amplitude of the displacement for the same driving field intensity (see Supporting Information for details). Using the experimentally measured FWM signal, we calculate $y(\omega_a)$ as 3×10^{-3} nm. From the electrostriction theory, we estimate $y(0)$ as 6.09×10^{-9} nm (see Supporting Information for details). This implies a quality factor of 5×10^5 – four orders of magnitude larger than viscoelastic theory predicts. This supports the hypothesis that bubbles are forming around the nanoparticles allowing them to oscillate with high quality factors.

Past works on nanoparticles²⁶ have suggested intrinsic damping factors of below 100; however, those works still included acoustic coupling to a substrate. Many possible mechanisms were suggested for this internal damping, including capping layers and crystal defects. Quality factors exceeding 10,000 have been reported for nanomechanical resonators²⁷. Those resonators were still coupled mechanically to the environment through an anchor point. Therefore, we believe that the intrinsic quality factor is still open for investigation, and our work suggests that large values can be found for nanoparticles if the damping from the surrounding environment is suppressed. The gold nanoparticles are expected to be single crystal since they are only 2 nm in size.

In summary, we have observed the “turning on” of unusually strong FWM scattering from nanoparticles in solution that extends above 1 THz. The strong FWM occurs at the resonances predicted by Lamb’s theory, so it may be attributed to elastic vibrations. Interestingly, the FWM signal does not obey the usual quadratic dependence, but shows a clear threshold at which the nonlinearity suddenly “turns on”. This indicates a phase transition, such as the formation of a cavity around the nanoparticles that reduces the damping. Theoretical analysis of the FWM process also suggests that much higher quality factors are required to see the observed signal than would be present usually in solution.

This new physics of high quality nanomechanical oscillations in solution has the potential for applications such as high bandwidth optical wavelength conversion with over THz wavelength shifting as desired optical wavelength division multiplexing²⁸⁻²⁹, or the spectroscopy of vibrational resonances of nanoparticles in solution. It is interesting to consider that this approach may be extended to probe the vibrational resonances of proteins – for example, the large scale elastic motions in the 100 GHz to THz range³⁰.

ASSOCIATED CONTENT

* Supporting Information: Detailed theory of nonlinear interaction and molecular dynamics simulations are provided.

The Supporting Information is available free of charge on the [ACS Publications website](#) at DOI: [xxxxxxx](#).

AUTHOR INFORMATION

Corresponding Author

* Email: rgordon@uvic.ca.

Funding

This work is supported by the NSERC CREATE grant Materials for Enhanced Energy Technologies.

ACKNOWLEDGMENT

The authors acknowledge funding from the Materials for Enhanced Energy Technologies NSERC CREATE program and the NSERC Discovery Grant program.

REFERENCES

- (1) Dhar, L.; Rogers, J. A.; Nelson, K. A. *Chem. Rev.* **1994**, 94, 157-193.
- (2) Ruhman, S.; Joly, A. G.; Nelson, K. A. *J. Chem. Phys.* **1987**, 86, 6563-6565.
- (3) Pelton, M.; Sader, J. E.; Burgin, J.; Liu, M.; Guyot-Sionnest, P.; Gosztola, D. *Nature Nanotech.* **2009**, 4, 492-495.
- (4) Juvé, V.; Crut, A.; Maioli, P.; Pellarin, M.; Broyer, M.; Del Fatti, N.; Vallée, F. *Nano Lett.* **2010**, 10, 1853-1858.
- (5) Crut, A.; Maioli, P.; Del Fatti, N.; Vallée, F. *Physics Reports*, **2015**, 549, 1-43.
- (6) Zijlstra, P.; Tchebotareva, A. L.; Chon, J. W.; Gu, M.; Orrit, M. *Nano Lett.* **2008**, 8, 3493-3497.
- (7) Marty, R.; Arbouet, A.; Girard, C.; Mlayah, A.; Paillard, V.; Lin, V. K.; Teo, S. L.; Tripathy, S. *Nano Lett.* **2011**, 11, 3301-3306.
- (8) Mongin, D.; Juvé, V.; Maioli, P.; Crut, A.; Del Fatti, N.; Vallée, F.; Sánchez-Iglesias, A.; Pastoriza-Santos, I.; Liz-Marzán, L. M. *Nano Lett.* **2011**, 11, 3016-3021.
- (9) Chakraborty, D.; van Leeuwen, E.; Pelton, M.; Sader, J. E. *J. Phys. Chem. C* **2013**, 117, 8536-8544.
- (10) O'Brien, K.; Lanzillotti-Kimura, N. D.; Rho, J.; Suchowski, H.; Yin, X.; Zhang, X. *Nature Commun.* **2014**, 5, 4042.
- (11) van Dijk, M. A.; Lippitz, M.; Orrit, M. *Phys. Rev. Lett.* **2005**, 95, 267406.
- (12) Hartland, G. V. *Annu. Rev. Phys. Chem.* **2006**, 57, 403-430.
- (13) Bragas, A. V.; Aku-Leh, C.; Costantino, S.; Ingale, A.; Zhao, J.; Merlin, R. *Phys. Rev. B* **2004**, 69, 205306.
- (14) Turton, D. A.; Senn, H. M.; Harwood, T.; Laphorn, A. J.; Ellis, E. M.; Wynne, K. *Nature Commun.* **2014**, 5, 3999.
- (15) Smith, P. W.; Ashkin, A.; Tomlinson, W. J. *Opt. Lett.* **1981**, 6, 284-286.
- (16) Lamb, H. *Proc. London Math. Soc.* **1881**, 1, 189-212.
- (17) Lide, D. R. *CRC Handbook of Chemistry and Physics*; CRC Press: Boca Raton, 2004.

- (18) Boyd, R. W. *Nonlinear Optics*, 3rd ed.; Academic Press: San Diego, 2008.
- (19) Saviot, L.; Netting, C. H.; Murray, D. B. *J. Phys. Chem. B* **2007**, 111, 7457-7461.
- (20) Agrawal, G. P. *Nonlinear fiber optics*, 5th ed.; Academic Press: San Diego, 2013.
- (21) Brennen, C. E. *Fundamentals of multiphase flow*; Cambridge University Press: Cambridge, 2005.
- (22) Akhatov, I.; Lindau, O.; Topolnikov, A.; Mettin, R.; Vakhitova, N.; Lauterborn, W. *Phys. Fluids* **2001**, 13, 2805-2819.
- (23) Buchner, R.; Barthel, J.; Stauber, J. *Chem. Phys. Lett.* **1999**, 306, 57-63.
- (24) McNamara, W. B.; Didenko, Y. T.; Suslick, K. S. *Nature* **1999**, 401, 772-775.
- (25) Beckett, M. A.; Hua, I. *J. Phys. Chem. A* **2001**, 105, 3796-3802.
- (26) Ruijgrok, P. V.; Zijlstra, P.; Tchegotareva, A. L.; Orrit, M. *Nano Lett.* **2012**, 12, 1063-1069.
- (27) Feng, X. L.; He, R.; Yang, P.; Roukes, M. L. *Nano Lett.* **2007**, 7, 1953-1959.
- (28) Geraghty, D. F.; Lee, R. B.; Verdiell, M.; Ziari, M.; Mathur, A.; Vahala, K. J. *IEEE J. Sel. Topics Quantum Electron.* **1997**, 3, 1146-1155.
- (29) Cotter, D.; Manning, R. J.; Blow, K. J.; Ellis, A. D.; Kelly, A. E.; Nasset, D.; Phillips, I. D.; Poustie, A. J.; Rogers, D. C. *Science* **1999**, 286, 1523-1528.
- (30) Tirion, M. M. *Phys. Rev. Lett.* **1996**, 77, 1905-1908.

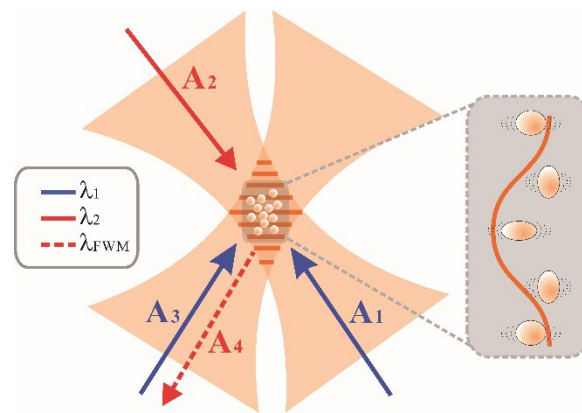


Figure aside abstract

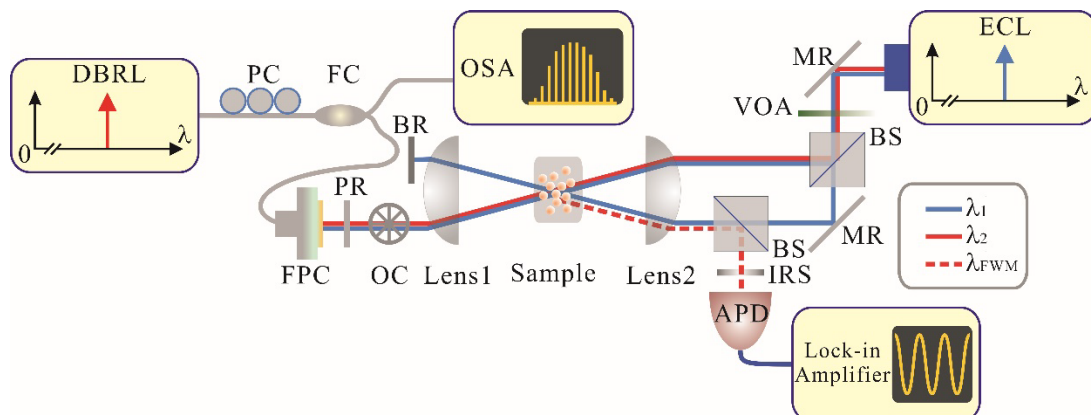


Figure 1. Experimental configuration of FWM. DBRL: distributed Bragg reflector laser; PC: polarization controller; FC: fiber coupler; OSA: optical spectrum analyzer; BR: blocker; FPC:

fiber-port collimator; PR: polarizer; OC: optical chopper; IRS: iris; APD: avalanche photodetector; BS: beam splitter; MR: mirror; VOA: variable optical attenuator; ECL: external cavity laser.

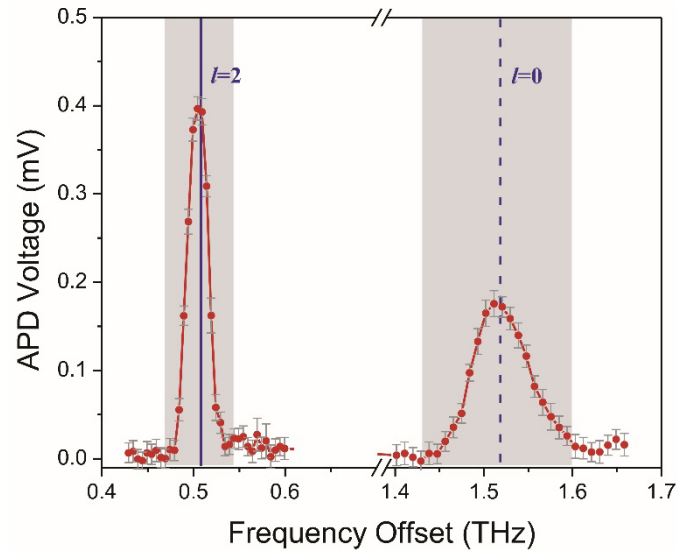


Figure 2. Four-wave mixing signal collected on avalanche photodiode (background Rayleigh scattering subtracted) for dilute 2 nm gold nanoparticles in water. Peaks at 504 GHz and 1.511 THz correspond to the $l=2$ and 0 acoustic vibrations of 2 nm gold spheres in vacuum. The distribution with 8% dispersion in particle diameter is shown with grey shading.

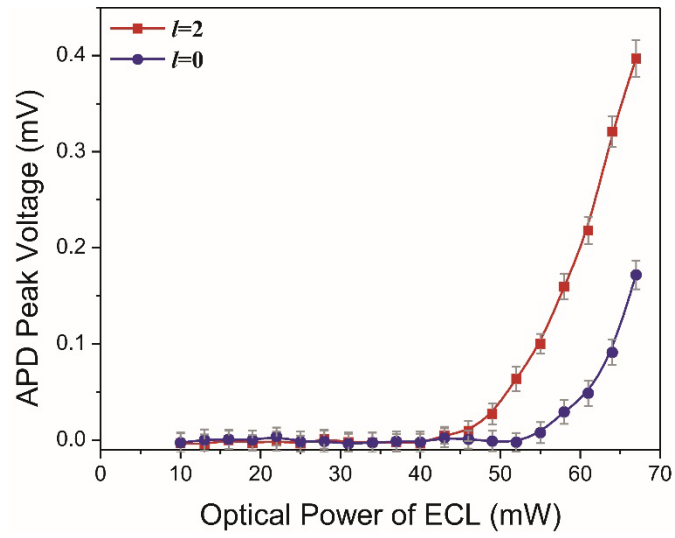


Figure 3. Power dependence of four-wave mixing signal observed on the avalanche photodiode for the $l=0$ (blue) and $l=2$ (red) peaks. A clear threshold is observed above which the nonlinear response “turns on”.